



Lennox, A. J. J., Fischer, S., Jurrat, M., Luo, S. P., Rockstroh, N., Junge, H., Ludwig, R., & Beller, M. (2016). Copper-Based Photosensitisers in Water Reduction: A More Efficient in Situ Formed System and Improved Mechanistic Understanding. *Chemistry - A European Journal*, 22(4), 1233-1238.  
<https://doi.org/10.1002/chem.201503812>

Peer reviewed version

Link to published version (if available):  
[10.1002/chem.201503812](https://doi.org/10.1002/chem.201503812)

[Link to publication record in Explore Bristol Research](#)  
PDF-document

This is the author accepted manuscript (AAM). The final published version (version of record) is available online via WILEY at <https://onlinelibrary.wiley.com/doi/abs/10.1002/chem.201503812> . Please refer to any applicable terms of use of the publisher.

## University of Bristol - Explore Bristol Research

### General rights

This document is made available in accordance with publisher policies. Please cite only the published version using the reference above. Full terms of use are available:  
<http://www.bristol.ac.uk/red/research-policy/pure/user-guides/ebr-terms/>

# Copper-Based Photosensitizers in Water Reduction: a More Efficient *in situ*-formed System and Improved Mechanistic Understanding

Alastair J. J. Lennox,<sup>[a]</sup> Steffen Fischer,<sup>[b]</sup> Mark Jurrat,<sup>[a]</sup> Shu-Ping Luo,<sup>[c]</sup> Nils Rockstroh,<sup>[a]</sup> Henrik Junge,<sup>[a]</sup> Ralf Ludwig,<sup>[b]</sup> Matthias Beller<sup>\*[a]</sup>

**Abstract:** The reduction of water has been achieved through a non-noble metal based homogeneous catalyst system that is formed *in situ*. Optimisation of the ligand quantities increased catalyst turnover numbers compared to pre-formed complexes. Mechanistic studies confirm a heteroleptic Cu complex as the active photosensitizer (PS) and an *in situ* formed Fe-phosphido dimer complex as the water reduction catalyst. The *in situ* method has been used to screen a range of ligands for the active PS, which has provided a number of structural features important to longevity and performance.

Transfer to a “hydrogen economy”<sup>[1]</sup> is considered a viable solution to prevent the well-documented negative effects associated with the rate of our fossil fuel consumption. Presently, H<sub>2</sub> is generated *via* steam reformation of fossil fuels themselves, thereby rendering the whole process ineffectual in its original objectives. Sustainable generation of this energy-dense and clean-burning gas, using renewable energy and materials, must therefore be realised.<sup>[2,3]</sup> Towards this end, solar-promoted water-splitting has become a hugely popular research endeavour,<sup>[4–8]</sup> from which the exploitation of homogeneous photocatalysis has experienced particular success,<sup>[9–11]</sup> especially in the utilisation of visible light, in contrast to the vast volume of literature on UV-absorbing semiconductor-based heterogeneous systems.<sup>[12–14]</sup>

There is a class of molecular systems that are composed of three-components and linked through a cascade.<sup>[15]</sup> They are originally inspired by nature, where reduction equivalents are generated by light in combination with coupled redox cycles in photosystems II and I.<sup>[16,17]</sup> An organometallic photosensitizer (PS) complex can be excited with visible light by a metal-to-ligand-charge-transfer ( $d \rightarrow \pi^*$ ), which undergoes electron transfer to a water reduction catalyst (WRC) and from a sacrificial reductant (SR). The reduced WRC can then reduce aqueous protons to liberate hydrogen gas, Figure 1. Due to their high redox potentials and activity under visible light irradiation, PSs based on Ru<sup>[18–20]</sup> and Ir<sup>[21–24]</sup> have become popular choices. However, despite numerous advances, there remain very significant, fundamental limitations that restrict the utility of this technology. One such limitation is the cost and complexity of the

catalysts employed, which has prompted the birth of cheap non-noble metal systems.<sup>[25–28]</sup> In 2013, we demonstrated that, in the presence of an iron-based WRC, heteroleptic Cu complexes, containing a bidentate phosphine and a phenanthroline ligand, behaved as suitable photosensitizers for proton reduction reactions.<sup>[29,30]</sup> These Cu-based complexes exhibit long excited-state lifetimes and a wide, ligand-dependent, range of reduction potentials.<sup>[30]</sup> We previously found evidence for both oxidative and reductive quenching pathways of the excited state, Figure 1.<sup>[31]</sup>

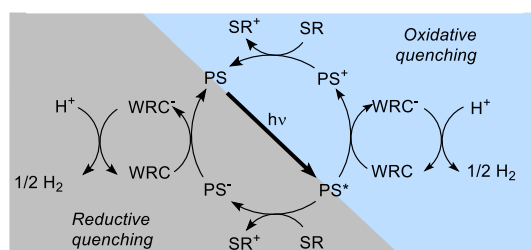


Figure 1: The two possible pathways in the generalized homogeneous photocatalytic cascade mechanism for the reduction of protons to H<sub>2</sub> gas. PS = photosensitizer, WRC = water reduction catalyst, SR = sacrificial reductant.

The Cu PS complexes are prepared *via* a two-step synthesis involving an over-night reflux, followed by a second reflux and a recrystallization. In order to improve the system, bypassing the synthesis of the organometallic complex is necessary to render the process operationally simpler and therefore time and cost effective. In addition, it would provide a facile method by which a broad range of ligands could be tested in order to establish a more stable and active system, whilst rapidly learning about the important structural features. Towards this end, a model system was identified, composed of a simple copper salt ([Cu(MeCN)<sub>4</sub>]PF<sub>6</sub>, (**1**)), a bidentate phosphine ligand (xantphos (**2a**)), a phenanthroline derivative previously known to be effective in harvesting light (bathocuproine (**3a**)) and a WRC precursor ([Fe<sub>3</sub>(CO)<sub>12</sub>] (**4**)), see Figure 2, right. Employing equimolar amounts of each component, it was established that upon their dissolution in THF and water, with the addition of a sacrificial reductant (NEt<sub>3</sub>) and subsequent visible light irradiation, H<sub>2</sub> could be generated in comparable volumes to the use of a molecularly defined, pre-formed, PS, Figure 2. This confirmed that rapid and selective formation of the active PS complex occurs *in situ*. Analysis of the generated gas mixture showed the presence of >98% H<sub>2</sub> with small (<0.4%) quantities of CO dissociating from the WRC.

When the catalyst components were added as solids to the flask, followed by the solvent mixture, the system was found to be very sensitive and reproducibility was poor. The use of stock solutions for each reacting component allowed for a more controlled and accurate addition of each species and the reproducibility was improved. However, the catalyst activity, longevity and decay rates were found to be dependent on the order of their addition. This interesting observation was initial

[a] Dr. A. J. J. Lennox, M. Jurrat, Dr. N. Rockstroh, Dr. H. Junge, Prof. Dr. M. Beller

Leibniz Institute for Catalysis at the University of Rostock,  
Albert Einstein-Straße 29a, 18059 Rostock, Germany  
E-mail: Matthias.beller@catalysis.de

[b] S. Fischer and Prof. Dr. R. Ludwig  
Institute of Chemistry, Department Physical Chemistry, University of  
Rostock, Dr. Lorenz-Weg 1, 18059 Rostock, Germany

[c] Dr. S. P. Luo,  
State Key Laboratory Breeding Base of Green Chemistry-Synthesis  
Technology,  
Zhejiang University of Technology, 310014 Hangzhou, China

Supporting information for this article is given via a link at the end of the document.

evidence of the multiple processes occurring in solution and their relative rates. The most dramatic effect occurred when bathocuproine (**3a**) was added at the very end, as no H<sub>2</sub> was formed, possibly indicating a competitive complexation to Cu from the SR. In addition, it was observed that higher volumes of gas were produced when the phosphine was mixed with copper before addition of bathocuproine (**3a**).<sup>[32]</sup> The most reliable and active system arose from the addition of bathocuproine (**3a**) after allowing xantphos (**2a**) and copper (**1**) to pre-mix, followed by NEt<sub>3</sub>, water and finally the addition of the [Fe<sub>3</sub>(CO)<sub>12</sub>] (**4**) complex.

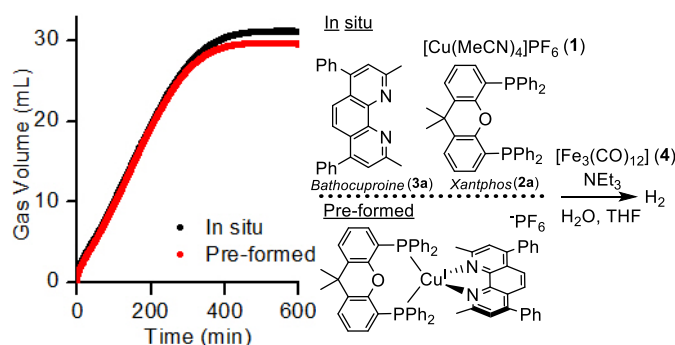


Figure 2: Gas evolution curves from the use of pre-formed (red) and *in situ* formed (black) catalyst systems

Previous mechanistic studies spectroscopically detected (*operando* FT-IR) a new iron dimer (**5**) under the reaction conditions, Figure 3.<sup>[31]</sup> With a bridging diphenylphosphido moiety, it closely resembles the efficient iron-based hydrogenase water reduction catalysts.<sup>[16,27,33,34]</sup> Proposed to be a resting state in the catalytic cycle of water reduction, the formation of this species was assumed to arise from oxidative decomposition of the phosphine-containing heteroleptic PS, by a derivative of the iron trimer precatalyst. Taking into account this phosphine consumption, and the possibility of further ligand degradation, the *in situ* system should allow for higher activities and longer catalyst lifetimes, as the equivalents of each reacting component can be varied. Keeping the concentration of **1** constant, the quantities of **2a**, **3a** and **4**, were all systematically varied, and the quantity and rate of H<sub>2</sub> generation was assessed. Due to the interconnection of the two catalysts and no clear single expensive component to optimise the system towards, it is most logical to judge the efficiency through the system turnover number, *i.e.* the combination of catalyst turnover numbers ( $\text{TON}_{\text{sys}} = \text{TON}_{\text{Cu}}^{\text{H}} + \text{TON}_{\text{Fe}}^{\text{H}_2}$ ).<sup>[35]</sup> Indeed, optimisation of ligand equivalents, Figure 3, provided almost an additional 30% of activity ( $\text{TON}_{\text{sys}} = 1050$  (unoptimised) vs 1330 (optimised)). The highest activity was observed using equimolar amounts of **1** and **2a** in combination with an excess of **3a** (1.5 equiv.) and substoichiometric quantities of **4** (0.7 equiv.), Figure 3.

An increase in the relative amount of phosphine ligand induces a negative effect on the catalyst activity, Figure 3, a fact that is surprising considering its apparent extra necessity in formation of the proposed active WRC and its role in forming the

assumed active heteroleptic copper PS ( $[\text{Cu}(\mathbf{2a})(\mathbf{3a})]^+$ ) complex. Additionally, the highest  $\text{TON}_{\text{sys}}$  comes from employing an excess of bathocuproine. It is well known there exists an equilibrium between copper heteroleptic, *e.g.*  $[\text{Cu}(\mathbf{2a})(\mathbf{3a})]^+$  and homoleptic, *e.g.*  $[\text{Cu}(\mathbf{3a})_2]^+$ , complexes,<sup>[36]</sup> and thus it seems entirely plausible from the evidence presented thus far that the excess of **3a** serves to favour the equilibrium in the direction of a homoleptic complex ( $[\text{Cu}(\mathbf{3a})_2]^+$ ) that is active, as observed in other applications.<sup>[37,38]</sup> Thus, the role of **2a** would be to provide a phosphido fragment to form the active Fe-dimer (**5**) WRC. In order to rationalise the optimised conditions and to aid further optimisations, mechanistic investigations were conducted with the first aim to elucidate the identity of the active PS and WRC species.

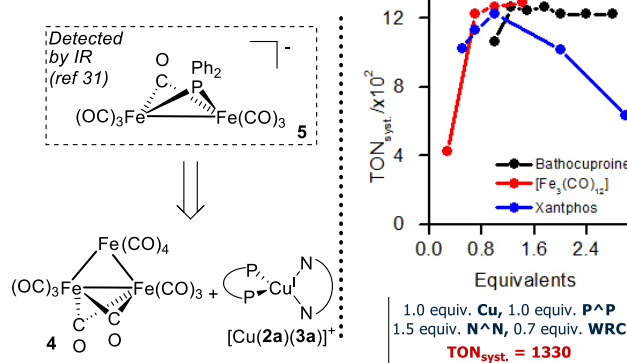


Figure 3: Left: The previously proposed resting state detected by *operando* FT-IR spectroscopy, which is assumed to be formed from reaction between the iron pre-catalyst **4**, or derivative thereof, and the heteroleptic  $[\text{Cu}(\mathbf{2a})(\mathbf{3a})]$ . Right: variation of the quantities of the catalyst components in the reduction of protons to H<sub>2</sub> gas. General conditions:  $[\text{Cu}(\text{MeCN})_4]\text{PF}_6$  (**1**) (3.5  $\mu\text{mol}$ , 1.3 mg, 1 equiv.), THF (10 mL), NEt<sub>3</sub> (3.75 mL) and water (1.25 mL), Xe lamp (input 300W, output 1.5 W). Xantphos (**2a**) variation: **3a** (2 equiv.) and **4** (0.7 equiv.); bathocuproine (**3a**) variation: **2a** (1 equiv.) and **4** (0.7 equiv.); Fe-trimer (**4**) variation: **3a** (2 equiv.), **2a** (1 equiv.).

In order to establish the dominant species in solution, the equilibrium ( $K_{\text{eq}}$ ) between the homoleptic ( $[\text{Cu}(\mathbf{3a})_2]^+$ ) and heteroleptic ( $[\text{Cu}(\mathbf{2a})(\mathbf{3a})]^+$ ) complexes, Figure 4, was studied.  $K_{\text{eq}}$  was measured (<sup>1</sup>H NMR) in a range of solvents. In DCM, CH<sub>3</sub>CN, acetone and in THF there was no, or very little, evidence of  $[\text{Cu}(\mathbf{3a})_2]^+$  formation. There was evidence for  $[\text{Cu}(\mathbf{3a})_2]^+$  in MeOH, but, surprisingly, in CDCl<sub>3</sub> the equilibrium lies almost entirely towards it. In the reaction solvent, (THF:NEt<sub>3</sub>:H<sub>2</sub>O 4:3:1) the equilibrium constant was measured (ESI-MS) as 0.29, meaning that over 65% of Cu exists as  $[\text{Cu}(\mathbf{2a})(\mathbf{3a})]^+$ . By changing the addition order of the ligands to copper, the rate of equilibration was found to be relatively slow. When **3a** was pre-mixed with **1** before addition of **2a**, the equilibrium favoured  $[\text{Cu}(\mathbf{3a})_2]^+$  by a further 6%, which readjusted over a period of 24 hours in the dark, or 2 hours of light irradiation. When this addition order was followed under catalytic conditions, the activity of the system dropped. This evidence provides the first hints that the homoleptic complex, which is formed in a greater proportion when bathocuproine (**3a**) is added before copper, is *not* the active PS species. The influence of visible light on  $K_{\text{eq}}$  was also tested (<sup>1</sup>H NMR) in D<sub>8</sub>-THF and found to effect a shift towards  $[\text{Cu}(\mathbf{3a})_2]^+$ . This is

consistent with previous electrochemical studies that show a progressive build-up of homoleptic complex upon redox cycling,<sup>[31]</sup> and thus light induced excitation is shown here to effect the same process.

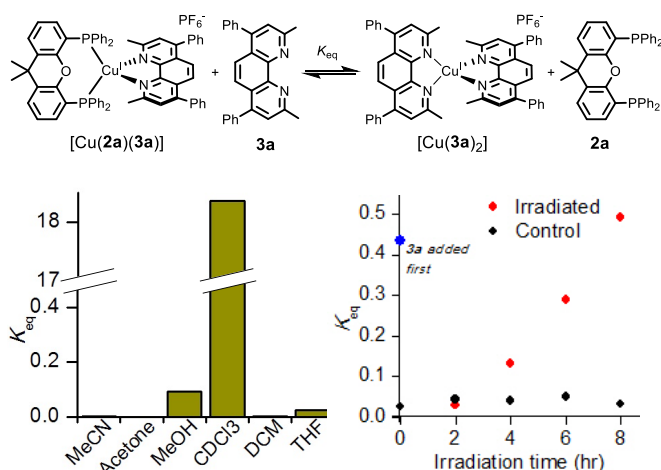


Figure 4: Equilibrium between  $[\text{Cu}(\mathbf{2a})(\mathbf{3a})]^+$  and  $[\text{Cu}(\mathbf{3a})_2]^+$ , showing the equilibrium constant ( $K_{\text{eq}}$ ), left, in different solvents, right, changing under the effect of light irradiation (Xe-lamp, output: 1.5 W) in a THF solution.

Having established that  $[\text{Cu}(\mathbf{2a})(\mathbf{3a})]^+$  is the species in highest concentration, it was important to establish their relative reactivity, due to the possibility of a small proportion of highly reactive PS responsible for the observed activity. To do this, it was necessary to confirm that the observed Fe phosphido-bridged dimer (**5**) is an active species. Thus **5** was independently synthesized,<sup>[39]</sup> and tested in combination with pre-formed  $[\text{Cu}(\mathbf{2a})(\mathbf{3a})]^+$  and compared to the use of precatalyst trimer **4**. When ensuring the same number of Fe atoms are present, the same volume of  $\text{H}_2$  was observed, Figure 5, thereby confirming the role of **5** as an active WRC. This is consistent with previous studies that have shown improved activities with the addition of monodentate tris[3,5-bis(trifluoromethyl)phenyl] phosphine to  $[\text{Fe}_3(\text{CO})_{12}]$  (**4**) in combination with a preformed stable Ir-based PS.<sup>[40]</sup> Addition of the same phosphine to this Cu-based system resulted no significant increase in activity.

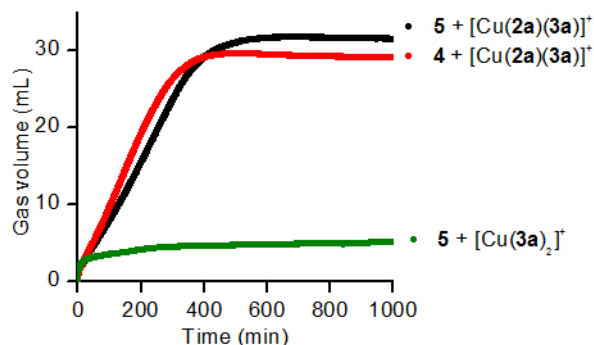


Figure 5: Gas evolution curves for (black dots) synthesized Fe-dimer **5** with heteroleptic  $[\text{Cu}(\mathbf{2a})(\mathbf{3a})]^+$ , (red dots) Fe-trimer **4** with heteroleptic  $[\text{Cu}(\mathbf{2a})(\mathbf{3a})]^+$  and (green dots) Fe-dimer **5** with homoleptic  $[\text{Cu}(\mathbf{3a})_2]^+$ .

Despite this evidence strongly suggesting that  $[\text{Cu}(\mathbf{2a})(\mathbf{3a})]^+$  is the active PS, the possibility of its disproportionation to form homoleptic  $[\text{Cu}(\mathbf{3a})_2]^+$  means this cannot be directly confirmed. However, when **5** was used in combination with  $[\text{Cu}(\mathbf{3a})_2]^+$ , in a system with no available bidentate phosphine ligand, no gas was evolved, thereby confirming  $[\text{Cu}(\mathbf{2a})(\mathbf{3a})]^+$  as the active PS. This is consistent with the excited-state lifetime of the homoleptic complex being orders of magnitude shorter than the heteroleptic complex,<sup>[30,42]</sup> which renders the kinetic requirement of electron transfer much more demanding.

A drawback of the homogeneous systems is their limited activity, as  $\text{H}_2$  gas production levels out as catalyst degradation proceeds. A progressive build-up of black precipitate and the detection of CO by GC provide evidence for dissociation of the Fe-stabilising CO ligand and subsequent agglomeration of Fe atoms. Attempts to prolong activity through the addition of slow-releasing CO agents, such as  $\text{Mo}(\text{CO})_6$  and PhCHO, unfortunately failed. Concurrent quantitative monitoring of the WRC by *operando* IR analysis of the  $\text{C}\equiv\text{O}$  stretch and  $\text{H}_2$  evolution showed the presence of **5** after gas evolution had ceased.<sup>[32]</sup> This evidence implies that WRC **5** outlives the PS co-catalyst. Indeed,  $\text{TON}_{\text{sys}}$  is higher employing sub-stoichiometric quantities of **4**, because then it cannot quantitatively destroy all  $[\text{Cu}(\mathbf{2a})(\mathbf{3a})]^+$ , when converting its phosphine to **5**.

In order to gain a handle on all system components, it was necessary to combine the *operando* IR with a technique suitable for simultaneously monitoring the PS concentration. Due to the positively charged copper complex, ESI-MS (positive ion-mode) was ideal, as it has proven use in detecting sensitive reaction intermediates.<sup>[43,44]</sup> Thus, with periodic sampling for ESI analysis and quantification through external calibration before and after every sample, the developed *operando* IR/*ex situ* ESI technique provided all information necessary, Figure 6. An initial rise in the concentration of  $[\text{Cu}(\mathbf{3a})_2]^+$  was observed due to light irradiation, as explained by Figure 4. However, it gradually decays whilst  $[\text{Cu}(\mathbf{2a})(\mathbf{3a})]^+$  remains relatively stable. Upon consumption of  $[\text{Cu}(\mathbf{3a})_2]^+$ , rapid degradation of  $[\text{Cu}(\mathbf{2a})(\mathbf{3a})]^+$  then ensues. This indicates that **3a** dissociation is a major PS degradation pathway and that  $[\text{Cu}(\mathbf{3a})_2]^+$  serves as a reservoir of **3a** to regenerate  $[\text{Cu}(\mathbf{2a})(\mathbf{3a})]^+$  through adjustment of its equilibrium. This may explain why using an increased proportion of **3a** provides higher  $\text{TON}_{\text{sys}}$ . Plotting the rate of gas evolution versus both the concentration of  $[\text{Cu}(\mathbf{2a})(\mathbf{3a})]^+$  and **5** allowed for a quantitative assessment of the catalyst degradation pathways.<sup>[32]</sup> In both cases, linear relationships were recorded, but the y-intercept only crossed 0 with  $[\text{Cu}(\mathbf{2a})(\mathbf{3a})]^+$ , i.e. **5** was still present despite the activity having already ceased. In combination with analysis of the gas evolution curves, these data suggest the degradation of the catalysts are linked to each other but led by the PS through decoordinative loss of **3a**. A clear first order decay of **5** ensues *after* initiation of the rapid degradation of  $[\text{Cu}(\mathbf{2a})(\mathbf{3a})]^+$ . **5** is stabilised by catalytic turn-over, but when this starts to attenuate due to PS degradation, CO loss and Fe agglomeration follows.

A series of control reactions were undertaken to further understand the mechanism for the formation of **5**. C-P bond cleavage in aryl phosphines has been well studied<sup>[41a-e]</sup> and used.<sup>[41f,g,h]</sup> As it has been shown to readily occur under



reductive conditions (e.g. with alkali metals<sup>[41d,e]</sup>) we suspected the formation of  $\text{PPh}_2^-$  to be highly influenced by reduction equivalents produced by the combination of a PS and the TEA electron source. Indeed, after 5 hr of light irradiation on solutions deficient in either CuPS or TEA, no evidence (IR) of **5** formation was provided. An extremely attenuated build-up of **5** was in fact observed in the absence of CuPS, but the time scale was far extended beyond that observed under the optimized conditions. In the absence of TEA, all Fe complexes had been consumed after 4 hr, but none of which were **5**.<sup>[32]</sup> Thus, reductive C-P cleavage in xantphos provides the anionic  $\text{PPh}_2^-$  fragment, which coordinates to a dimeric Fe carbonyl complex to yield dimer **5**.

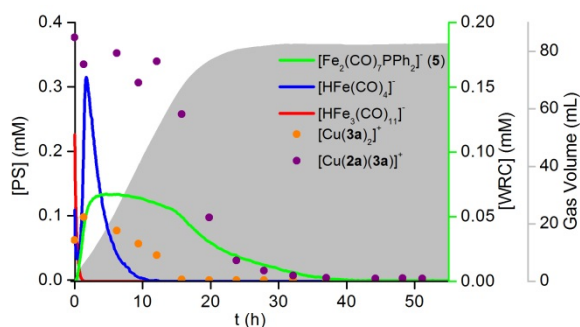


Figure 6: Operando IR/ex-situ ESI measurements showing concentrations of Fe species (coloured lines) and Cu complexes (blue dots – heteroleptic  $[\text{Cu}(\mathbf{2})(\mathbf{3a})]^+$  and grey dots homoleptic  $[\text{Cu}(\mathbf{3a})_2]^+$ ). Shaded area indicates gas volume evolved. Conditions:  $[\text{Cu}(\text{MeCN})_4]\text{PF}_6$  (7  $\mu\text{mol}$ ), xantphos (7  $\mu\text{mol}$ ), bathocuproine (10.5  $\mu\text{mol}$ ),  $[\text{Fe}_3(\text{CO})_{12}]$  (5  $\mu\text{mol}$ ), THF:NEt<sub>3</sub>:H<sub>2</sub>O (4:3:1, 20 mL).

With an optimised model system in hand and mechanistic understanding enhanced, the *in situ* method was exploited to explore variation of the bidentate phosphine (**2**), to establish the important features pertinent to this parameter. The HOMO of the heteroleptic complex  $[\text{Cu}(\mathbf{2})(\mathbf{3a})]^+$  is not purely localized on Cu, but contains a substantial portion of phosphine character.<sup>[42a]</sup> Thus, the phosphine moiety can modify the electronic structure and stabilise the excited state. 32 different ligands were tested under the optimised conditions, the majority of which are bidentate phosphines (**2a-w**),<sup>[32]</sup> but also a small number of BIANs (**6**), phosphites (**7**) and NHCs (**8**) were tested. A sample was removed at the start for ESI-MS analysis to determine the  $[\text{Cu}(\mathbf{2})(\mathbf{3a})]^+ / [\text{Cu}(\mathbf{3a})_2]^+$  ratio. From the gas evolution curves, it was immediately obvious that the rate of H<sub>2</sub> production,  $\text{TON}_{\text{sys}}$ , and lifetime of the system are all dependent on the phosphine ligand.<sup>[32]</sup> The rate differs dramatically, which could be evidence for a change in the dominant quenching mechanism, Figure 1. In addition, the percentage of heteroleptic PS is also very sensitive to the nature of the phosphine, as previously observed by Armaroli and co-workers.<sup>[36]</sup> Plotting this % against  $\text{TON}_{\text{sys}}$  reveals the important influence of  $[\text{Cu}(\mathbf{2})(\mathbf{3a})]^+$ , and is directly consistent with our mechanistic studies. With a greater proportion of the active complex, and thus a lower  $K_{\text{eq}}$ , higher turn-over numbers are achieved, Figure 7.

Table 1. A selection of ligands tested in the developed *in-situ* system.<sup>[32]</sup>

| Ligand <sup>[a]</sup> | Vol H <sub>2</sub> / mL <sup>[b]</sup> | $\text{TON}_{\text{sys}}$ <sup>[c]</sup> | % Heteroleptic <sup>[d]</sup> |
|-----------------------|--|--|-------------------------------|
|-----------------------|--|--|-------------------------------|

|                                      |      |      |    |
|--------------------------------------|------|------|----|
| Xantphos ( <b>2a</b> )               | 32.4 | 1335 | 65 |
| BISBI ( <b>2b</b> )                  | 19.5 | 760  | 65 |
| DPE-Phos ( <b>2c</b> )               | 27.3 | 1090 | 73 |
| DPMe-Phos ( <b>2d</b> )              | 20.4 | 780  | 25 |
| Bppm ( <b>2e</b> )                   | 13.7 | 470  | 17 |
| Dppb ( <b>2f</b> )                   | 5.0  | 155  | 45 |
| Xantphos- <i>t</i> -Bu ( <b>2g</b> ) | 5.2  | 120  | 14 |
| Thixantphos ( <b>2h</b> )            | 27.9 | 1130 | 57 |
| Dixantphos ( <b>2i</b> )             | 11.1 | 190  | 3  |
| Naphos ( <b>2j</b> )                 | 30.0 | 1220 | 37 |
| Naphos-CF <sub>3</sub> ( <b>2k</b> ) | 9.1  | 290  | 5  |

[a] See supporting information for reaction conditions and full list of ligands and their structures (**2a-w**); [b] Vol H<sub>2</sub> calculated by removing the blank volume (measured as 2.40 mL) and taking into account the % H<sub>2</sub> detected by GC (generally <98%); [c]  $\text{TON}_{\text{sys}} = \text{TON}_{\text{Cu}^{\text{I}}} + \text{TON}_{\text{Fe}^{\text{H}_2}}$ ; [d] TON rounded to nearest 5. [d] remaining Cu is all homoleptic complex,  $[\text{Cu}(\mathbf{3})_2]^+$

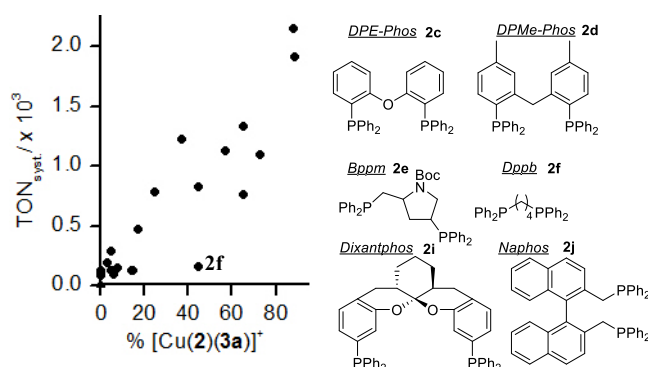


Figure 7. Left:  $\text{TON}_{\text{sys}}$  vs %  $[\text{Cu}(\mathbf{2})(\mathbf{3a})]^+$ , where the remaining copper is all homoleptic complex  $[\text{Cu}(\mathbf{3})_2]^+$ , and right: structures of some diphosphines tested.

Many of the efficient phosphines contain a bridging O-atom, which may play a role in stabilising the excited state through a hemi-labile coordination. Comparison of %  $[\text{Cu}(\mathbf{2})(\mathbf{3a})]^+$  for DPE-Phos (**2c**) and DPMPhos (**2d**) suggests that bridging-O aids in increasing the proportion of heteroleptic complex and thus the  $\text{TON}_{\text{sys}}$ . Changing the electronics and/or the bulk at phosphorous will also have an effect on the proportion of  $\text{PS}_{\text{hetero}}$  present. Switching phenyl for *any* substituent in the xantphos or naphos range resulted in lower or no heteroleptic complex formation, which is reflected in lower catalytic activities, Figure 7 and Table 1. This implies a balanced electron demand is ideal for high activity.

However, the vertical spread of activity between the points of similar %  $[\text{Cu}(\mathbf{2})(\mathbf{3a})]^+$  proves it is not the only important parameter. This was further demonstrated by subjecting a pure preformed heteroleptic complex, with dppp (**2q**) and **3a** ligated to Cu,  $[\text{Cu}(\mathbf{2})(\mathbf{3a})]^+$ ,<sup>[45]</sup> to the reaction conditions and observing no gas evolution. Knör and Monkowius provided a model that

showed increasing bite angles stabilise the HOMO by reducing the orbital overlap between ligand and metal. This effect will widen the redox potential and increase the thermodynamic driving force, which may provide a rationale for the ineffectual alkyl phosphines with a small bite-angle. However, comparison between bppm (**2e**) and dppb (**2f**), which share the same bite angle and similar electronic properties at phosphorus also reveal the importance of a rigid backbone. The flexible dppb (**2f**) is the major outlier in Figure 7, as it forms good proportions of heteroleptic complex but shows much lower activity than bppm (**2e**), which is restricted by a cyclized backbone. This may also be the reason for a lower activity observed in the case of dixantphos (**2i**), which is a more flexible variant of xantphos (**2a**). In addition to the increased orbital overlap aided by increased flexibility in the diphosphine, it is likely that a greater degree of flattening to a square planar complex occurs upon excitation. This process leads to shorter lifetimes through solvent-induced exciplex quenching.<sup>[30,46]</sup> Thus, like sterics, rigidity can restrict the distortion away from a *pseudo*-tetrahedron and stabilise the excited state.

Replacing the methyl groups at the 2,9-positions of bathocupoine (**3a**) with increasing bulk provides increasingly more active systems and correlate nicely to Taft's steric parameter.<sup>[32]</sup> This is consistent with the use of preformed complexes, whose excited-state lifetimes were measured and found to rise with increasing bulk.<sup>[30]</sup> Using the *in situ* system, it was found that the ratio of  $[\text{Cu}(\mathbf{2})(\mathbf{3})]^+$  to  $[\text{Cu}(\mathbf{3})_2]^+$  (ESI-MS) also rises with increasing bulk in the 2,9-positions of bathocupoine. Thus, the increased life time and concentration of active PS both contribute to the greater observed rates. The use of stabilising NHC or phosphite (**7**) ligands in combination with the light harvesting bathocupoine showed no ability to generate H<sub>2</sub> gas. Monodentate NHC leads to a trigonal planar complex, which is particularly vulnerable to non-radiative decay pathways.<sup>[47]</sup> Additionally, replacing the bathocupoine completely with a BIAN (**6**) ligand in combination with phosphine predictably showed no activity.

In summary we have demonstrated a viable solution to the problem of the organometallic complex synthesis in non-noble metal water reduction systems. Optimisation of the quantity of ligands led to improvements in the system efficiency. Synthesis of the dimeric iron WRC **5** established it to be the active species. In combination with studies on the homoleptic/heteroleptic equilibrium, the heteroleptic  $[\text{Cu}(\mathbf{2a})(\mathbf{3a})]^+$  was also confirmed to be the active PS. The dominant degradation pathway was elucidated through monitoring the reaction by *operando* IR/*in situ* ESI and involves destruction of the active  $[\text{Cu}(\mathbf{2a})(\mathbf{3a})]^+$ , which is likely caused through loss of the **3a** unit. The ease of catalyst preparation by the *in situ* system allowed for further rapid exploration of the system. A large range of alternative ligands for Cu were screened and the proportion of  $[\text{Cu}(\mathbf{2})(\mathbf{3})]^+$ , *i.e.*  $K_{\text{eq}}$ , was found to be integral for high activities. Additionally, a rigid backbone, wide bite angle and balanced electronic properties at phosphorus were all found to be important. These data provide rationale for future optimisations in the PS and the WRC.

## Acknowledgements

A.J.J.L. would like to thank the Alexander von Humboldt Foundation for generous funding. This work was also supported by the Ministry for Education, Science and Culture of Mecklenburg Vorpommern and the European Union (Investing in our Future, European Regional Development) within the project PS4H and a joint DFG/NFSC project. We would like to thank Andreas Koch for assistance with the quantitative ESI measurements, E. Oberem and A. Rösel for preparation of compound **5**<sup>[39]</sup> and Dr A. Spannenberg for X-ray crystallography.

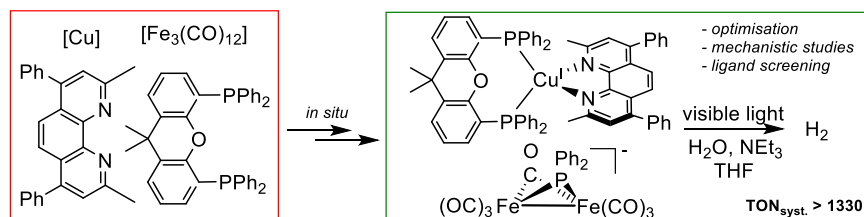
**Keywords:** homogeneous catalysis • photocatalysis • reduction • reaction mechanisms • copper

- [1] J. O. Bockris, *Science* **1972**, *176*, 1323.
- [2] J. A. Turner, *Science* **2004**, *305*, 972–974.
- [3] T. R. Cook, D. K. Dogutan, S. Y. Reece, Y. Surendranath, T. S. Teets, D. G. Nocera, *Chem. Rev.* **2010**, *110*, 6474–6502.
- [4] T. Hisatomi, J. Kubota, K. Domen, *Chem. Soc. Rev.* **2014**, *43*, 7520–7535.
- [5] K. Maeda, *J. Photochem. Photobiol. C* **2011**, *12*, 237–268.
- [6] K. S. Joya, Y. F. Joya, K. Ocakoglu, R. van de Krol, *Angew. Chem. Int. Ed.* **2013**, *52*, 10426–10437.
- [7] M. Ashokkumar, *Int. J. Hydrogen Energy* **1998**, *23*, 427–438.
- [8] V. Balzani, A. Credi, M. Venturi, *ChemSusChem* **2008**, *1*, 26–58.
- [9] A. J. Esswein, D. G. Nocera, *Chem. Rev.* **2007**, *107*, 4022–4047.
- [10] M. A. Gross, A. Reynal, J. R. Durrant, E. Reisner, *J. Am. Chem. Soc.* **2014**, *136*, 356–366.
- [11] J. J. Concepcion, R. L. House, J. M. Papanikolas, T. J. Meyer, *Proc. Natl. Acad. Sci. USA* **2012**, *109*, 15560–15564.
- [12] X. Chen, S. Shen, L. Guo, S. S. Mao, *Chem. Rev.* **2010**, *110*, 6503–6570.
- [13] Y. Ma, X. Wang, Y. Jia, X. Chen, H. Han, C. Li, *Chem. Rev.* **2014**, *114*, 9987–10043.
- [14] A. L. Linsebigler, G. Lu, J. T. Yates, *Chem. Rev.* **1995**, *95*, 735–758.
- [15] W. T. Eckenhoff, R. Eisenberg, *Dalton Trans.* **2012**, *41*, 13004–13021.
- [16] A. Magnuson, M. Anderlund, O. Johansson, P. Lindblad, R. Lomoth, T. Polivka, S. Ott, K. Stensjö, S. Styring, V. Sundström, L. Hammarström, *Acc. Chem. Res.* **2009**, *42*, 1899–1909.
- [17] S. Styring, *Faraday Discuss.* **2012**, *155*, 357–376.
- [18] K. Kalyanasundaram, J. Kiwi, M. Graetzel, *Helv. Chim. Acta* **1978**, *61*, 2720–2730.
- [19] G. C. Vougioukalakis, A. I. Philippopoulos, T. Stergiopoulos, P. Falaras, *Coord. Chem. Rev.* **2011**, *255*, 2602–2621.
- [20] A. Abbotto, N. Manfredi, *Dalton Trans.* **2011**, *40*, 12421–12438.
- [21] J. I. Goldsmith, W. R. Hudson, M. S. Lowry, T. H. Anderson, S. Bernhard, *J. Am. Chem. Soc.* **2005**, *127*, 7502–7510.
- [22] B. F. DiSalle, S. Bernhard, *J. Am. Chem. Soc.* **2011**, *133*, 11819–21.
- [23] F. Gärtner, D. Cozzula, S. Losse, A. Boddien, G. Anilkumar, H. Junge, T. Schulz, N. Marquet, A. Spannenberg, S. Gladiali, M. Beller, *Chem. Eur. J.* **2011**, *17*, 6998–7006.
- [24] F. Gärtner, S. Denurra, S. Losse, A. Neubauer, A. Boddien, A. Gopinathan, A. Spannenberg, H. Junge, S. Lochbrunner, M. Blug, S. Hoch, J. Busse, S. Gladiali, M. Beller, *Chem. Eur. J.* **2012**, *18*, 3220–3225.
- [25] P. Du, R. Eisenberg, *Energy Environ. Sci.* **2012**, *5*, 6012–6021.
- [26] Y. Amao, T. Hirakawa, N. Himeshima, *Catal. Commun.* **2008**, *9*, 131–134.
- [27] S. Tschierlei, S. Ott, R. Lomoth, *Energy Environ. Sci.* **2011**, *4*, 2340–2352.
- [28] P. Poddutoori, D. T. Co, A. P. S. Samuel, C. H. Kim, M. T. Vagnini, M. R. Wasielewski, *Energy Environ. Sci.* **2011**, *4*, 2441–2450.

- 
- [29] S.-P. Luo, E. Mejía, A. Friedrich, A. Pazidis, H. Junge, A.-E. Surkus, R. Jackstell, S. Denurra, S. Gladiali, S. Lochbrunner, M. Beller, *Angew. Chem. Int. Ed.* **2013**, 52, 419–423.
- [30] E. Mejía, S.-P. Luo, M. Karnahl, A. Friedrich, S. Tschierlei, A.-E. Surkus, H. Junge, S. Gladiali, S. Lochbrunner, M. Beller, *Chem. Eur. J.* **2013**, 19, 15972–15978.
- [31] S. Fischer, D. Hollmann, S. Tschierlei, M. Karnahl, N. Rockstroh, E. Barsch, P. Schwarzbach, S.-P. Luo, H. Junge, M. Beller, S. Lochbrunner, R. Ludwig, A. Brückner, *ACS Catal.* **2014**, 4, 1845–1849.
- [32] See SI for more details.
- [33] D. Streich, Y. Astuti, M. Orlandi, L. Schwartz, R. Lomoth, L. Hammarström, S. Ott, *Chem. Eur. J.* **2010**, 16, 60–63.
- [34] W. Lubitz, E. J. Reijerse, J. Messinger, *Energy Environ. Sci.* **2008**, 1, 15–31.
- [35] As the photosensitizer undergoes two turnovers per H<sub>2</sub> formed, the TON is calculated for H rather than H<sub>2</sub>, *i.e.*,  $\text{TON}_\text{H} = n\text{H}/n\text{Cu}$ . Whereas, Fe undergoes one turnover per H<sub>2</sub> formed as is thus calculated for H<sub>2</sub>, *i.e.*  $\text{TON}_{\text{H}_2} = n\text{H}_2/n\text{Fe}$
- [36] A. Kaeser, M. Mohankumar, J. Mohanraj, F. Monti, M. Holler, J.-J. Cid, O. Moudam, I. Nierengarten, L. Karmazin-Brelot, C. Duhayon, B. Delavaux-Nicot, N. Armaroli, J.-F. Nierengarten, *Inorg. Chem.* **2013**, 52, 12140–12151.
- [37] D. R. McMillin, K. M. McNett, *Chem. Rev.* **1998**, 98, 1201–1220.
- [38] D. V. Scaltrito, D. W. Thompson, J. A. O'Callaghan, G. J. Meyer, *Coord. Chem. Rev.* **2000**, 208, 243–266.
- [39] B. Walther, H. Hartung, H.-C. Böttcher, U. Baumeister, U. Böhlend, J. Reinhold, J. Sieler, J. Ladriere, H.-M. Schiebel, *Polyhedron* **1991**, 10, 2423–2435.
- [40] F. Gärtner, A. Boddien, E. Barsch, K. Fumino, S. Losse, H. Junge, D. Hollmann, A. Brückner, R. Ludwig, M. Beller, *Chem. Eur. J.* **2011**, 17, 6425–6436.
- [41] a) P. E. Garrou, *Chem. Rev.* **1985**, 85, 171–185, b) K. Q. Almeida Lenero, Y. Guari, P. C. J. Kamer, P. W. N. M. van Leeuwen, B. Donnadieu, S. Sabo-Etienne, B. Chaudret, M. Lutz, A. L. Spek, *Dalton Trans.* **2013**, 42, 6495–6512, c) C. W. Bradford, R. S. Nyholm, *J. Chem. Soc., Dalton Trans.* **1973**, 529–533, d) A. M. Aguiar, J. Beisler, A. Mills, *J. Org. Chem.* **1961**, 27, 1001–1005; e) I. Toth, B. E. Hanson, M. E. Davis, *Organometallics* **1990**, 9, 675–680, f) K. F. Crespo Andrada, L. E. Peisino, M. Güney, A. Daştan, A. B. Pierini, *Org. Biomol. Chem.* **2013**, 11, 955–965, g) M. W. Bezpalko, B. M. Foxman, C. M. Thomas, *Inorg. Chem.* **2013**, 52, 12329–12331, h) V. A. Stepanova, V. V. Dunina, I. P. Smoliakova, *Organometallics* **2009**, 28, 6546–6558.
- [42] a) A. K. Ichinaga, J. R. Kirchhoff, D. R. McMillin, C. O. Dietrich-Buchecker, P. A. Marnot, J. P. Sauvage, *Inorg. Chem.* **1987**, 26, 4290–4292, b) A. Kaeser, O. Moudam, G. Accorsi, I. Séguy, J. Navarro, A. Belbakra, C. Duhayon, N. Armaroli, B. Delavaux-Nicot, J.-F. Nierengarten, *Eur. J. Inorg. Chem.* **2014**, 2014, 1345–1355.
- [43] L. S. Santos, C. H. Pavam, W. P. Almeida, F. Coelho, M. N. Eberlin, *Angew. Chem. Int. Ed.* **2004**, 43, 4330–4333.
- [44] G. W. Amarante, H. M. S. Milagre, B. G. Vaz, B. R. Vilachã Ferreira, M. N. Eberlin, F. Coelho, *J. Org. Chem.* **2009**, 74, 3031–3037.
- [45] T. Tsubomura, K. Kimura, M. Nishikawa, T. Tsukuda, *Dalton Trans.* **2015**, 44, 7554–7562.
- [46] S. Tschierlei, M. Karnahl, N. Rockstroh, H. Junge, M. Beller, S. Lochbrunner, *ChemPhysChem* **2014**, 15, 3709–3713.
- [47] V. A. Krylova, P. I. Djurovich, M. T. Whited, M. E. Thompson, *Chem. Commun.* **2010**, 46, 6696–6698.
-

---

## Table of Contents



### Copper-Based Photosensitizers in Water Reduction: a More Efficient *in situ*-Formed System and Improved Mechanistic Understanding

Alastair J. J. Lennox,<sup>[a]</sup> Steffen Fischer,<sup>[b]</sup> Mark Jurrat,<sup>[a]</sup> Shu-Ping Luo,<sup>[c]</sup> Nils Rockstroh,<sup>[a]</sup> Henrik Junge,<sup>[a]</sup> Ralf Ludwig,<sup>[b]</sup> Matthias Beller<sup>\*,[a]</sup>

**Cheap n Easy H<sub>2</sub>:** The reduction of water has been achieved through a non-noble metal based homogeneous catalyst system that is formed *in situ*. Optimisation of the ligand quantities increased catalyst turnover numbers compared to pre-formed complexes. Mechanistic studies confirm a heteroleptic Cu complex as the active photosensitizer (PS) and an *in situ* formed Fe-phosphido dimer complex as the water reduction catalyst. The *in situ* method has been used to screen a range of ligands for the active PS, which has provided a number of structural features important to longevity and performance.